



Published in final edited form as:

*J Pharm Sci.* 2008 October ; 97(10): 4425–4432. doi:10.1002/jps.21325.

## Nanodisks Derived from Amphotericin B Lipid Complex

Megan Tuffeland<sup>1</sup>, Gang Ren<sup>2</sup>, and Robert O. Ryan<sup>1</sup>

<sup>1</sup>Center for Prevention of Obesity, Diabetes & Cardiovascular Diseases, Children's Hospital Oakland Research Institute, 5700 Martin Luther King Jr. Way, Oakland, California 94609

<sup>2</sup>Department of Biochemistry & Biophysics, University of California, San Francisco, 1700 4th Street, MC 2532, Byers Hall, Rm 301C, San Francisco, California 94158

### Abstract

The goal of this study was to determine the effect of apolipoproteins on Amphotericin B lipid complex (ABLC). We report that incubation of ABLC with recombinant human apolipoprotein A-I (apoA-I) induces solubilization of ABLC by transforming the micron sized phospholipid/AMB assemblies into discrete nanoscale disk-shaped complexes termed nanodisks (ND). ApoA-I induced changes in ABLC solubility and morphology were monitored by spectroscopy and electron microscopy. AMB efficacy was evaluated in yeast and pathogenic fungi growth inhibition assays and the effect of AMB formulation on cell toxicity was assessed in cultured Hep3B cells. AMB associated with ND were more efficiently nebulized than AMB associated with ABLC. Thus, transformation of ABLC into ND preserves the potent biological activity of AMB as well as the reduced toxicity of the ABLC formulation. ABLC derived AMB-ND offer advantages over conventional ABLC in terms of stability, storage, nebulization efficiency and provides an intrinsic "handle" for tissue specific targeting via genetic engineering of its protein component.

### Keywords

amphotericin B; amphotericin B lipid complex; nanoparticles; nanodisk; proteins; apolipoprotein A-I; phospholipid; aerosols; drug transport; solubility

## INTRODUCTION

The polyene antibiotic, amphotericin B (AMB), has been used clinically for nearly half a century. However, its therapeutic applications are limited by infusion-related toxicity and nephrotoxicity.<sup>1</sup> Research on this problem has led to development of three distinct AMB lipid formulations that show promise for the treatment of systemic fungal infections and leishmaniasis. Among the lipid formulations approved by the U.S. Food and Drug Administration for human use is amphotericin B lipid complex (ABLC; Abelcet<sup>TM</sup>). ABLC consists of a 1:1 weight ratio of AMB and the phospholipids, dimyristoylphosphatidylcholine (DMPC) and dimyristoylphosphatidylglycerol (7:3, w/w). Freeze fracture electron microscopy studies revealed that ABLC forms large ribbon-like sheets with diameters ranging from 1 to 10  $\mu\text{m}$ .<sup>2</sup> In aqueous media ABLC exists as an insoluble suspension of AMB and phospholipid.

Recently, we reported a novel lipid formulation of AMB wherein the antibiotic is incorporated into water-soluble, nanometer-scale reconstituted high-density lipoprotein like particles, termed nanodisks (ND).<sup>3</sup> AMB-ND are ternary complexes of phospholipid, AMB, and

apolipoprotein. ND formation takes advantage of the phospholipid reorganizing capability of members of the exchangeable apolipoprotein family. Human apolipoprotein A-I (apoA-I), for example, possesses the capacity to transform specific phospholipid vesicles into nanometer scale disk complexes.<sup>4</sup> These particles exist as a disk-shaped phospholipid bilayer whose edge is stabilized by interaction with amphipathic  $\alpha$ -helices of apolipoprotein molecules. In the case of complexes formed upon incubation of DMPC and apoA-I (2.5:1, w/w), each ND particle contains approximately 200 molecules of phospholipid and two apoA-I aligned anti-parallel in an extended “belt” like fashion around the perimeter of the disk-shaped bilayer.<sup>3,5</sup> Thus, otherwise exposed phospholipid fatty acyl chains at the disk edge are protected from exposure to the aqueous milieu, resulting in a stable complex. In the case of AMB containing ND, the product particles display potent *in vitro* and *in vivo* antifungal activity.<sup>3</sup> Recently, AMB-ND were shown to be highly effective against cutaneous *Leishmania major* infection in BALB/c mice.<sup>6</sup>

Based on the fact that phospholipids present in ABLC are known substrates for apolipoprotein induced self assembly of ND, we hypothesized that incubation of isolated recombinant apoA-I with ABLC would induce formation of AMB-ND. Potential advantages of a ND formulation versus ABLC include AMB solubility in aqueous media, discrete nanoscale particle size, storage capability in a lyophilized state, feasibility of aerosolization and potential for tissue specific targeting by engineering the protein component of ND. In the present study we report that apoA-I induces a rapid and complete transformation of ABLC into AMB-ND that retain the potent antifungal properties of ABLC.

## MATERIALS AND METHODS

### Materials

Recombinant apoA-I was produced as previously described.<sup>7</sup> ABLC and AMB-deoxycholate (Fungizone) were obtained from the In-patient Pharmacy at the Children’s Hospital and Research Center Oakland. AMB-deoxycholate was resuspended in sterile deionized water according to the manufacturer’s instructions. The 18 amino acid amphipathic peptide, 4F<sup>8</sup> was purchased from Celtek Biosciences (Nashville, TN).

### Analytical Procedures

ApoA-I concentration was determined by the bicinchoninic acid assay (Pierce Chemical Co., Rockford, IL) with bovine serum albumin as standard. AMB levels were determined using an extinction coefficient at 416 nm =  $1.214 \times 10^5 \text{ M}^{-1} \text{ cm}^{-1}$  in dimethylsulfoxide (DMSO).<sup>9</sup>

### ND Preparation

ABLC was gently agitated to disperse the settled mixture. One milliliter ABLC suspension (5 mg phospholipid, 5 mg AMB) and 0.4 mL apoA-I (5 mg/mL in PBS; 20 mM sodium phosphate, pH 7.4, 150 mM sodium chloride) were combined and the vessel flushed with N<sub>2</sub> gas, capped and subjected to bath sonication at 22°C for 40 min. The resulting solution was sterile filtered (0.22  $\mu\text{m}$ ) and stored at 4°C until use.

### AMB Solubility Studies

One milliliter dispersed ABLC (5 mg AMB) was combined with 0.4 mL PBS or PBS containing 5 mg/mL apoA-I and the samples bath sonicated for 40 min at 22°C. In a separate control incubation, ABLC was mixed with PBS but not sonicated. Following incubation/sonication, the samples were centrifuged at 9000g for 3 min and the AMB content in the supernatant determined.

### Negative Stain Electron Microscopy

Aliquots (2.5 ml) of ABLC or apoA-I solubilized ABLC were adhered to carbon-coated, 400-mesh copper grids previously rendered hydrophilic by glow discharge. The grids were washed for 1 min with three successive drops of deionized water and then exposed to three successive drops of 2% (w/v) uranyl nitrate for 1 min (Ted Pella, Tustin, CA). Images at 19000 $\times$  or 80000 $\times$  magnification were recorded on 4 K  $\times$  4 K Gatan UltraScan CCD under low electron dose conditions using a Tacnai 20 electron microscope (Philips Electron Optics/FEI, Eindhoven, The Netherlands) operating at 200 kV. Each pixel of the micrographs corresponds to 5.5 Å or 1.4 Å at the level of the specimen. Particles in micrographs were semi-automatically selected and boxed using EMAN software.<sup>10</sup> Each box size is 142 pixels, corresponding to 20 nm in specimen.

### UV/Vis Absorbance Spectroscopy

Absorbance spectroscopy was performed on a Perkin Elmer Lambda 20 spectrometer. Samples (12.4 mg/mL AMB) were scanned from 300 to 450 nm in PBS.

### Yeast Growth Inhibition Assays

Cultures of the yeast, *Saccharomyces cerevisiae*, were grown in yeast extract peptone glucose broth media (YEPD; Teknova, Hollister, CA). Twenty microliters of a saturated overnight culture was used to inoculate 5 mL YEPD media in the absence or presence of indicated amounts of a given AMB formulation. Cultures were grown for 20 h at 30°C with rotation and the extent of culture growth monitored by measuring sample turbidity at 600 nm.

### Pathogenic Fungi Growth Inhibition Assays

Microtiter broth growth inhibition assays were conducted with three species of pathogenic fungi, *Aspergillus fumigatus* (ATCC#: 16424), *Candida albicans* (ATCC #: 90028) and *Cryptococcus neoformans* (isolate H99, ATCC #: 208821). Fungi were cultured in RPMI 1640 medium buffered with MOPS to pH 6.8. The final inoculum was  $1 \times 10^4$  spores/mL (*A. fumigatus*),  $1 \times 10^4$  cells/mL (*C. albicans*), and  $2.5 \times 10^3$  cells/mL (*C. neoformans*). All experiments were performed in triplicate at 35°C for 48 h according to established protocols.<sup>11,12</sup> All samples tested were soluble in the standard RPMI medium used and no contamination, precipitation, or interference was seen in any of the samples tested against either fungal species. Growth inhibition activities of AMB containing samples were determined from cultures grown in the absence or presence of AMB (concentration range 0.0045–14  $\mu$ g/mL). Values for inhibitory concentration equal to or greater than 90% (IC<sub>90</sub>) were determined visually using a colorimetric indicator that changes hue in the presence of metabolically active organisms.

### Cell Culture Studies

Hep3B human hepatoma cells were grown in MEM (Gibco, Carlsbad, CA) supplemented with 4 mM L-glutamine, 0.1 mM nonessential amino acids, 1.0 mM sodium pyruvate, and 10% fetal bovine serum. Cells were split twice weekly into fresh medium and maintained at 37°C in a humidified 5% CO<sub>2</sub> atmosphere. For experiments, cells ( $2.2 \times 10^4$  cells per well) were seeded in 24-well plates in 1.0 mL complete medium. The medium was aspirated and replaced after 48 h at which time the cells were treated with a given AMB formulation at concentrations ranging from 0 to 20  $\mu$ g/mL. In other studies HEK293 cells were grown in DMEM supplemented with 10% fetal bovine serum. Cells were split twice weekly into fresh medium and maintained at 37°C in a humidified 5% CO<sub>2</sub> atmosphere. For experiments, cells ( $3.9 \times 10^5$  cells per well) were seeded in 24-well plates in 1.0 mL complete medium. After 24 h, the medium was aspirated and replaced by DMEM supplemented with 4% fetal bovine serum and Fungizone, ABLC or ABLC derived ND, (from 0 to 100  $\mu$ g AMB/mL). All assays were performed in triplicate. After 24 h culture in the presence or absence of antibiotic, cell viability

was measured spectrophotometrically using the 3-(4, 5-dimethylthiazolyl-2)-2, 5-diphenyltetrazolium bromide (MTT) assay as described by the manufacturer (Sigma). Values are expressed as percentages of absorbance of untreated control cells.

### **Nebulization Efficiency**

All measurements were performed in triplicate at ambient temperature. Initial nebulizer reservoir AMB concentration was 1 mg/mL with a starting volume of 5 mL. The jet nebulizer (Salter Labs, Arvin, CA) was attached to a variable autotransformer (Staco Energy Products, Dayton, OH) set at 90 V and the samples nebulized continuously for 20 min. The amount of AMB in the reservoir (mg AMB/mL solution) was measured before and after nebulization and used to determine nebulization efficiency.<sup>13,14</sup>

## **RESULTS**

### **ApoA-I Induced ABLC Solubilization**

Incubation of isolated recombinant human apoA-I with ABLC results in transformation of the sample from an insoluble lipid dispersion into a clarified, transparent yellow solution (Fig. 1). In control incubations lacking apoA-I, ABLC sample turbidity persists. To quantitate the extent of AMB solubilization, product samples were centrifuged at 9000g for 3 min. Following this an aliquot of the supernatant was transferred to a solution of DMSO and the AMB content determined spectrophotometrically (Tab. 1). In the control ABLC sample, negligible AMB was detected in the supernatant. Likewise, bath sonication of ABLC only marginally increased the amount of AMB recovered in the supernatant. By contrast, >99% of the AMB in ABLC was present in the supernatant fraction following incubation with apoAI. Based on results of previous studies<sup>3,15</sup> it was hypothesized that ABLC had been transformed into apolipoprotein stabilized ND particles. To examine this in greater detail, the spectroscopic and morphological characteristics of the reaction product were evaluated.

### **Absorbance Spectroscopy of AMB Lipid Complexes**

AMB displays characteristic spectral properties that report on the organizational state of the antibiotic.<sup>16</sup> Whereas UV/Vis absorbance spectra of monomeric AMB in organic solvent shows well resolved maxima at 416, 392, and 372 nm, the spectral properties of AMB in aqueous media are different and reflect the extent of antibiotic self association.<sup>15</sup> Spectra of control ABLC lack well-defined features owing to insolubility of this formulation in buffer (Fig. 2). On the other hand, the spectrum of apoA-I solubilized ABLC in PBS reveals prominent spectral maxima at 414, 385, 362, and 333, similar to that seen for AMB-ND prepared according to Oda et al.<sup>3</sup> and Hargreaves et al.<sup>15</sup>

### **Electron Microscopy**

Consistent with earlier freeze fracture electron micrographs of ABLC that revealed micron sized ribbon-like sheets of the lipid-drug complex,<sup>2</sup> negative stain electron microscopy of ABLC revealed large amorphous structures (Fig. 3). By contrast, following incubation with apoA-I and solubilization of ABLC, discrete particles were present that display a disk-like morphology similar to that reported for AMB-ND.<sup>3</sup> In the case of ABLC-derived ND, the average particle diameter was ~11 nm with a range from 7 to 20 nm (Fig. 3, panel C).

### **Biological Activity**

To determine the effect of apoA-I induced transformation of ABLC into ND on AMB biological activity, yeast growth inhibition studies were conducted (Fig. 4). The data, expressed as % maximal yeast growth, showed no differences between control ABLC and ABLC-derived AMB-ND. Both formulations showed 50% growth inhibition at 0.15 µg/mL AMB.

Furthermore, substitution of apoA-I with the 20 amino acid amphipathic peptide, 4F,<sup>8</sup> resulted in an ABLC-derived ND formulation that displayed growth inhibition properties indistinguishable from those observed with apoA-I derived ND (data not shown). Likewise, in pathogenic fungi growth inhibition assays the formulations were equivalent inhibitors of *C. albicans*, *A. fumigatus*, and *C. neoformans* growth (Tab. 2). These results corroborate previously published findings of both ABLC<sup>17</sup> and AMB-ND.<sup>3,8</sup> Previously, it was shown that apolipoproteins alone or empty ND lacking AMB have no antibiotic activity.<sup>3</sup>

### Tissue Culture Studies

To evaluate formulation dependent effects on AMB toxicity toward cultured cells, Hep3B cells were incubated with increasing amounts of AMB as ABLC, ABLC-derived ND, or AMB-deoxycholate (Fig. 5). In the case of AMB-deoxycholate, dramatic effects occurred at relatively low AMB concentrations with nearly 100% cell death at 10 µg/mL. On the other hand, cell growth was largely unaffected by exposure to ABLC or ABLC-derived AMB-ND. At all concentrations tested there was a <2% decrease in Hep3B cell viability. In other experiments with cultured HEK293 cells, cell proliferation was largely unaffected by incubation with 100 µg/mL AMB as ABLC or ABLC-ND. By contrast, cell viability was completely lost at this concentration of AMB deoxycholate (data not shown).

### Nebulization Efficiency

To assess the relative potential of ABLC and AMB-ND formulations for pulmonary delivery of the antibiotic, nebulization experiments were performed. Nebulization efficiency was estimated by measuring the AMB concentration in the solution remaining in the nebulizer reservoir after 20 min continuous nebulization. In both cases, the starting concentration of AMB was 1.0 mg/mL and the volume remaining in the nebulizer reservoir following nebulization was ~2 mL. In the case of AMB-ND, the concentration of AMB in the nebulizer reservoir was 1.07 ± 0.03 mg/mL, whereas AMB concentration of ABLC increased to 1.30 ± 0.07 mg/mL.

## DISCUSSION

Despite dramatic changes in morphology, AMB formulated into ND particles display biological activity indistinguishable from ABLC. While the *in vitro* studies reported here show no striking difference in biological activity, it may be predicted that effects observed *in vivo* may be beneficial. The large size of ABLC (1–10 µm) favors rapid clearance from blood and accumulation in organs rich in phagocytic cells, resulting in reduced antibiotic activity.<sup>18</sup> As demonstrated above, conversion of ABLC into ND may enhance AMB residence time in the circulation, potentially improving its therapeutic index.

ABLC is one of three distinct AMB lipid formulations approved for use in humans. Like AMB colloidal dispersion (Amphotec<sup>TM</sup>), a complex of AMB and cholesteryl sulfate,<sup>19</sup> and liposomal AMB (AmBisome<sup>TM</sup>), consisting of spherical liposomes containing hydrogenated soy phosphatidylcholine, cholesterol, distearoylphosphatidylglycerol, and AMB,<sup>20</sup> these formulations effectively decrease the dose-limiting toxicity of conventional AMB deoxycholate. In a similar manner, AMB-ND capitalize on the principle of a lipid carrier to achieve lower toxicity but, in addition, contain an apolipoprotein component that imparts intrinsic versatility to the vehicle. This concept is consistent with the finding of Wasan et al. 21 who reported that AMB associated with plasma high density lipoprotein displayed reduced toxicity.

Based on data obtained from studies of apolipoprotein-phospholipid interactions, the mechanism of ABLC-derived AMB-ND formation likely involves apolipoprotein dependent

disruption of the ribbon-like structures and reorganization of the components into discrete entities that are stabilized and solubilized through their interaction with apolipoprotein.<sup>22</sup> At the same time, it is evident that further studies are required to define the molecular details of this reaction. There are several reasons AMB-ND show promise for treatment of systemic fungal disease. For example, the protein component of ND may be engineered to introduce cell specific targeting signals while retaining its phospholipid solubilization activity.<sup>23</sup> Although inclusion of recombinant protein adds to production cost and is a potential source of bacterial toxins, it has been shown recently that apolipoprotein mimetic peptides, as small as 18 amino acids in length, can substitute for apolipoproteins as structural components of AMB-ND. ND prepared in such a manner may have advantages over ND formulated with recombinant protein in terms of clinical studies.<sup>8</sup> Beneficial features of AMB-ND in general include their ability to be lyophilized and reconstituted with preservation of ND particle structure and AMB biological activity (unpublished observations). This should increase shelf life and facilitate transportation at minimal cost. The soluble ABLC-derived AMB-ND formulation also permits uniform and homogeneous aliquots of stock solutions to be removed and, because of formulation clarity, appearance of a precipitate due to improper storage or handling can be readily detected. Improved nebulization efficiency is another important advantage of AMB-ND over ABLC and, perhaps, other lipid formulations of AMB. Indeed, it is generally recognized that solutions are delivered more effectively than suspensions which yield low efficiency upon aerosolization.<sup>24</sup> Inherent AMB-ND solubility in aqueous media permits facile manipulation of nebulization droplet size, potentially enhancing penetration deep into lung tissue, a known site of deadly *Aspergillus* spp. infection.<sup>25</sup> Future *in vivo* studies will be required to determine if ND particles provide a more efficacious AMB-delivery vehicle for treatment of pulmonary mycoses.

## CONCLUSION

Over the last few decades, the incidence of superficial and deep mycotic infections has continued to rise. As the available antifungal formulations are diverse in composition, extensive studies are required to optimize drug formulations for clinical use. The transformation of Amphotericin B Lipid Complex into nanodisks provides an internally consistent means to directly compare physical and biological properties such that the difference between these very distinct formulations can be systematically evaluated. Future *in vivo* studies and protein engineering experiments designed for targeted delivery of AMB ND should offer new opportunities to treat systemic fungal infections.

## Acknowledgments

This work was supported by a grant (AI-61354) from the National Institutes of Health. G.R. was supported by W.M. Keck foundation. The authors thank Xiao Shu and Mina Nikanjam for assistance with cell culture as well as Nora Trice for assistance with nebulization.

## REFERENCES

1. Dupont B. Overview of the lipid formulations of amphotericin B. *J Antimicrob Chem* 2002;49:31–36.
2. Janoff AS, Boni LT, Popescu MC, Minchey SR, Cullis PR, Madden TD, Taraschi T, Gruner SM, Shyamsunder E, Tate MW, Mendelsohn R, Bonner D. Unusual lipid structures selectively reduce the toxicity of amphotericin B. *Proc Natl Acad Sci USA* 1988;85:6122–6126. [PubMed: 3413081]
3. Oda MN, Hargreaves PL, Beckstead JA, Redmond KA, van Antwerpen R, Ryan RO. Reconstituted high-density lipoprotein enriched with the polyene antibiotic, amphotericin B. *J Lipid Res* 2005;47:260–267. [PubMed: 16314670]
4. Pownall HJ, Massey JB, Kusserow SK, Gotto AM. Kinetics of lipid-protein interactions: Interaction of apolipoprotein A-I from human plasma high density lipoproteins with phosphatidylcholines. *Biochemistry* 1978;17:1183–1188. [PubMed: 207309]

5. Martin DD, Budamagunta MS, Ryan RO, Voss JC, Oda MN. Apolipoprotein A-I assumes a “looped belt” conformation on reconstituted high density lipoprotein. *J Biol Chem* 2006;281:20418–20426. [PubMed: 16698792]
6. Nelson KG, Bishop JV, Ryan RO, Titus R. Nanodisk-associated amphotericin B clears Leishmania major cutaneous infection in susceptible BALB/c mice. *Antimicrob Agents Chemother* 2006;50:1238–1244. [PubMed: 16569834]
7. Ryan RO, Forte TM, Oda MN. Optimized bacterial expression of human apolipoprotein A-I. *Protein Exp Purif* 2003;27:98–103.
8. Tufteland M, Pesavento JB, Bermingham RL, Hoeprich PD Jr, Ryan RO. Peptide stabilized amphotericin B nanodisks. *Peptides* 2007;28:741–746. [PubMed: 17293004]
9. Bolard J, Legrand P, Heitz F, Cybulska B. One-sided action of amphotericin B on cholesterol-containing membranes is determined by its self-association in the medium. *Biochemistry* 1991;30:5707–5715. [PubMed: 2043613]
10. Ludtke SJ, Baldwin PR, Chiu W. EMAN: Semiautomated software for high-resolution single-particle reconstructions. *J Struct Biol* 1999;128:82–97. [PubMed: 10600563]
11. Pfaller MA, Barry AL. Evaluation of a novel colorimetric broth microdilution method for antifungal susceptibility testing of yeast isolates. *J Clin Microbiol* 1994;32:1992–1996. [PubMed: 7989555]
12. Tiballi RN, He X, Zarins LT, Revankar SG, Kauffman CA. Use of a colorimetric system for yeast susceptibility testing. *J Clin Microbiol* 1995;33:915–917. [PubMed: 7790460]
13. Wong-Beringer A, Lambros MP, Beringer PM, Johnson DL. Suitability of caspofungin for aerosol delivery: Physicochemical profiling and nebulizer choice. *Chest* 2005;128:3711–3716. [PubMed: 16304338]
14. Weber A, Morlin G, Cohen M, Williams-Warren J, Ramsey B, Smith A. Effect of nebulizer type and antibiotic concentration on device performance. *Pediatr Pulmonol* 1997;23:249–260. [PubMed: 9141110]
15. Hargreaves PL, Nguyen TS, Ryan RO. Spectroscopic studies of amphotericin B solubilized in nanoscale bilayer membranes. *Biochim Biophys Acta* 2006;1758:38–44. [PubMed: 16473324]
16. Ernst C, Grange J. Structure of amphotericin B aggregates as revealed by UV and CD spectroscopies. *Biopolymers* 1981;20:1575–1588.
17. Carrillo-Munoz AJ, Ruesga M, Brio S, del Valle O, Rodriguez V, Santos P, Hernandez-Molina JM, Canton E, Peman J, Guarro J, Quindos G. Comparison of in vitro Antifungal Activities of Amphotericin B Lipid Complex with Itraconazole against 708 Clinical Yeast Isolates and Opportunistic Moulds Determined by National Committee for Clinical Laboratory Standards Methods M27-A and M38-P. *Chemotherapy* 2002;48:224–231. [PubMed: 12476038]
18. Janknegt R, de Marie S, Bakker-Woudenberg IA, Crommelin DJ. Liposomal and lipid formulations of amphotericin B. *Clin Pharmacokinet* 1992;23:279–291. [PubMed: 1395361]
19. Boswell GW, Buell D, Bekersky I. AmBisome (liposomal amphotericin B): A comparative review. *J Clin Pharmacol* 1998;38:583–592. [PubMed: 9702842]
20. Adler-Moore JP, Proffitt RT. Development, characterization, efficacy and mode of action of AmBisome, a unilamellar liposomal formulation of amphotericin B. *J Liposome Res* 1993;3:429–450.
21. Wasan KM, Rosenblum MG, Cheung L, Lopez-Berestein G. Influence of lipoproteins on renal cytotoxicity and antifungal activity of amphotericin B. *Antimicrob Agents Chemother* 1994;38:223–227. [PubMed: 8192447]
22. Nguyen T-S, Weers PMM, Raussens V, Wang Z, Ren G, Sulchek T, Hoeprich PD Jr, Ryan RO. Amphotericin B induces interdigitation of apolipoprotein stabilized nanodisk bilayers. *Biochim Biophys Acta*. 2008
23. Kiss RS, Weers PM, Narayanaswami V, Cohen J, Kay C, Ryan RO. Structure-guided protein engineering modulates helix bundle exchangeable apolipoprotein properties. *J Biol Chem* 2003;278:21952–21959. [PubMed: 12684504]
24. O’Riordan TG. Formulations and nebulizer performance. *Respir Care* 2002;47:1305–1312. [PubMed: 12425745]
25. Yao Z, Liao W. Fungal respiratory disease. *Curr Opin Pulm Med* 2006;12:222–227. [PubMed: 16582678]

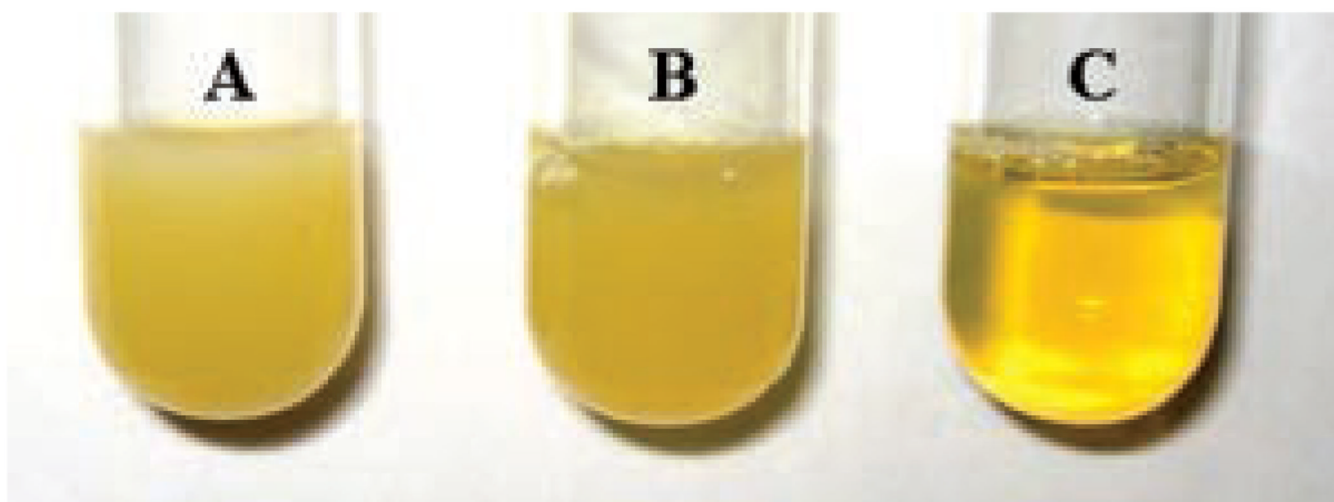


**Figure 1.** Effect of ApoA-I on the solubility/appearance of ABLC. (A) Control ABLC (1 mL) plus PBS (0.4 mL). (B) Bath sonicated ABLC plus PBS. (C) Bath sonicated ABLC plus PBS containing 5 mg/mL apoA-I.



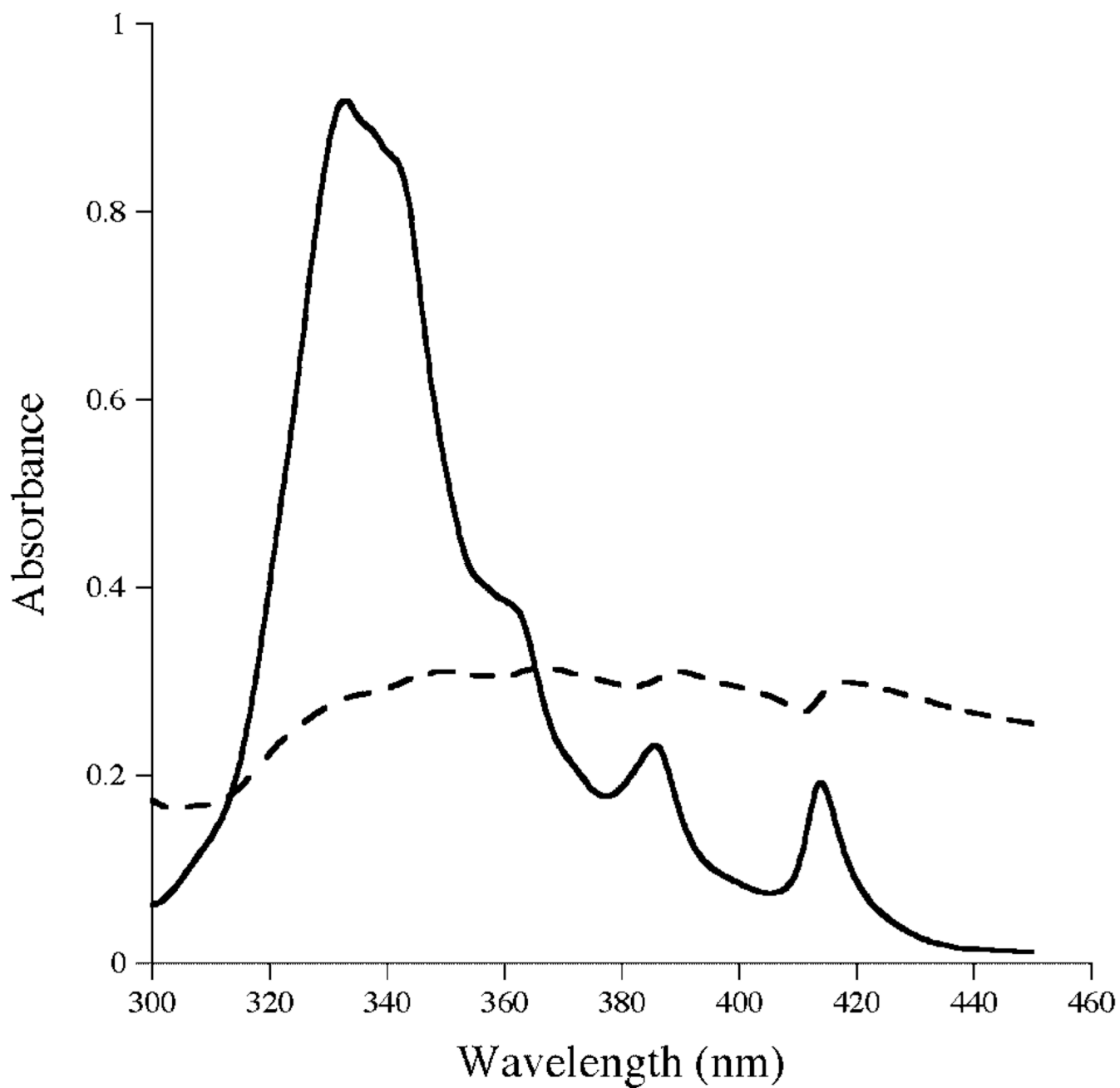


**Figure 2.** Spectroscopy of AMB samples. UV/Visible absorbance spectra of ABLC (dashed line) and apoA-I solubilized ABLC (solid line). Samples (12.4  $\mu\text{g}$  AMB/mL) were scanned from 300 to 450 nm.

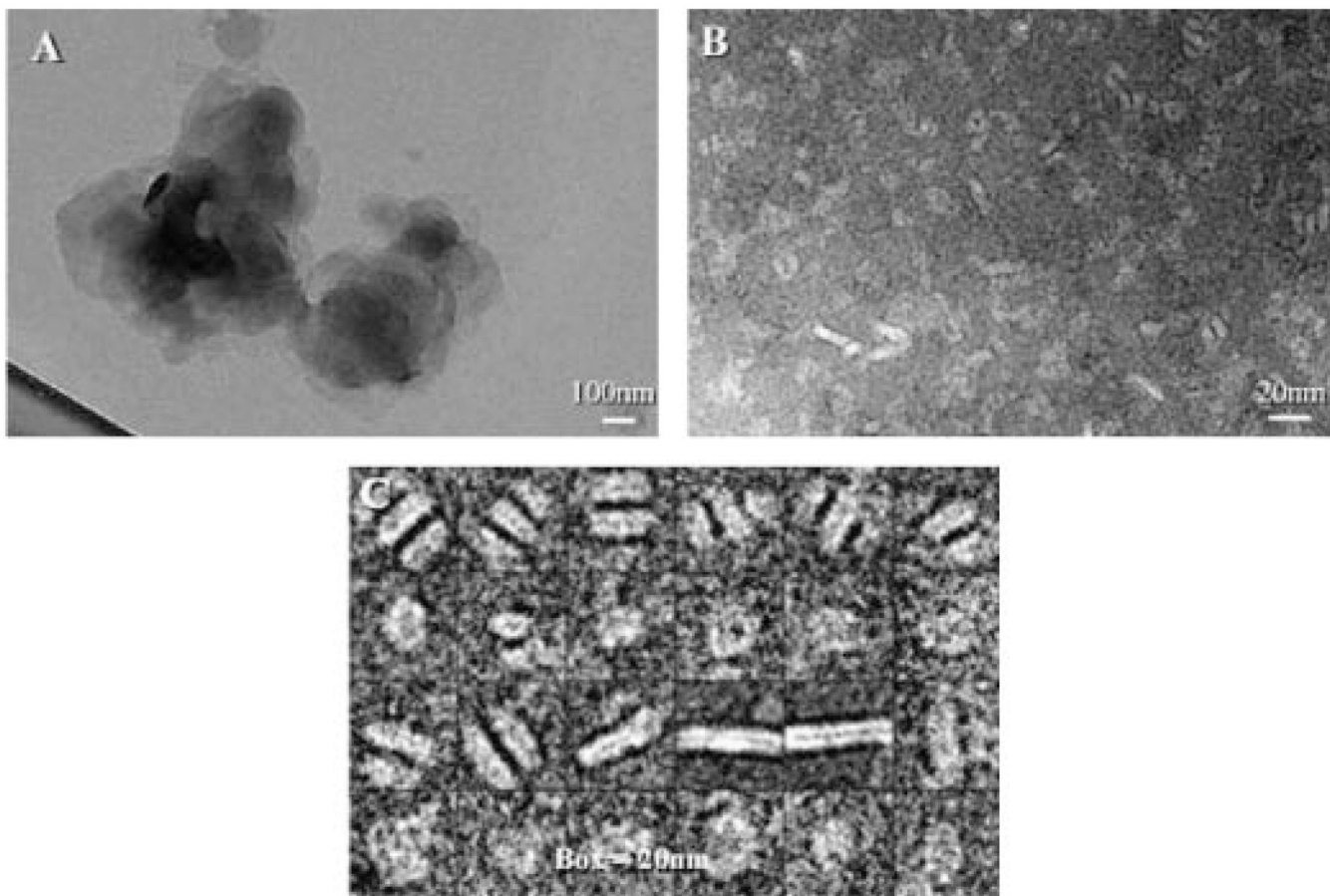


**Figure 3.** Electron Microscopy of AMB preparations. Negative stain electron micrographs of ABLC alone (Panel A), ApoA-I solubilized ABLC (Panel B). Panel C depicts selected images from Panel B (note the different size scales for each panel).

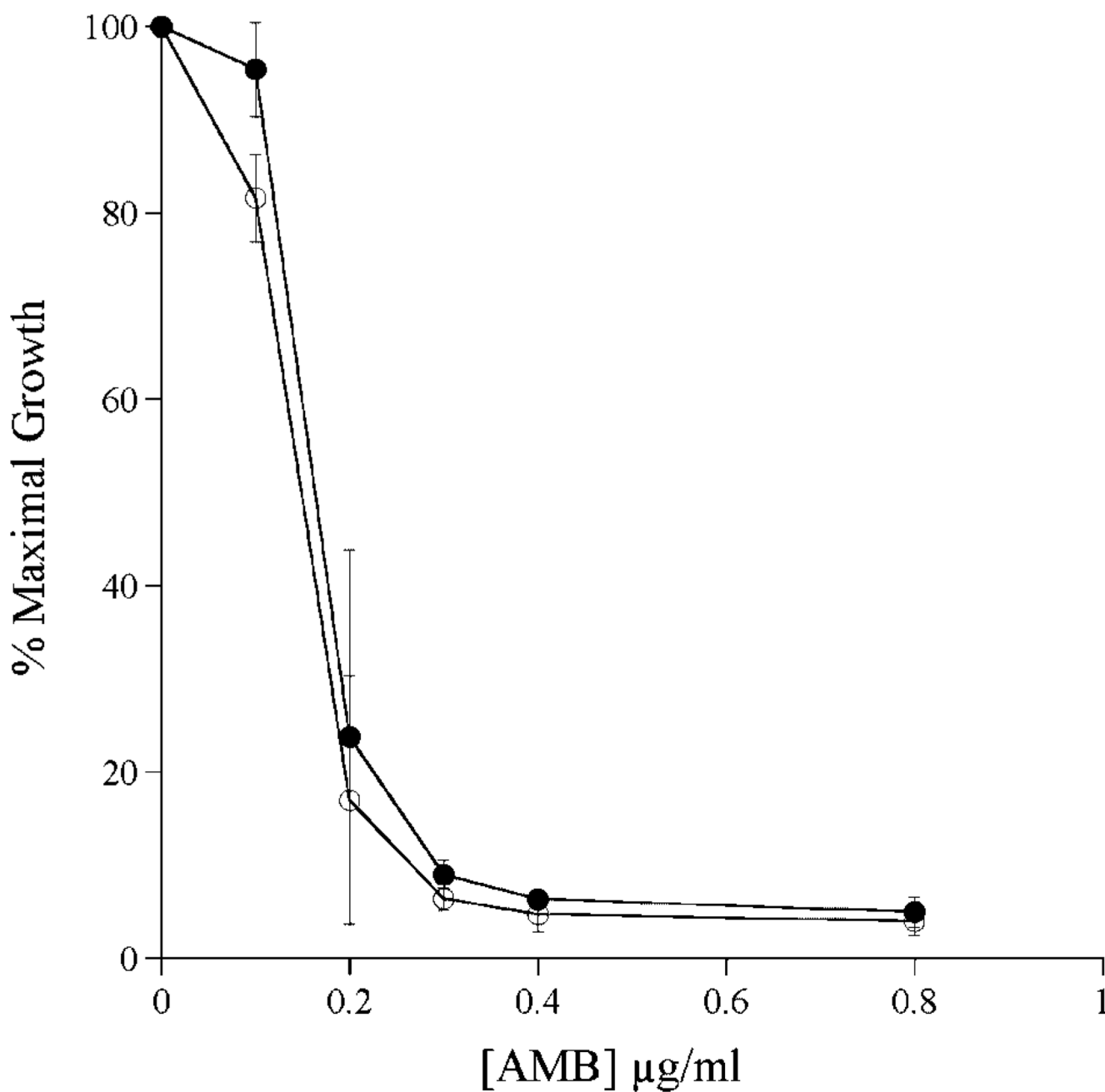


**Figure 4.** Effect of ABLC and ABLC derived ND on growth of *Sacchaormyces cerevisiae*. Twenty microliters of a saturated overnight culture was used to inoculate 5 mL YEPD media in the absence or presence of indicated amounts of ABLC or ABLC-derived ND. Cultures were grown for 20 h at 30°C with rotation and the extent of culture growth monitored by measuring sample turbidity at 600 nm. (Filled circles) control ABLC; (open circles) ABLC-derived AMB-ND. Values reported are the mean  $\pm$  SD ( $n = 3$ ).

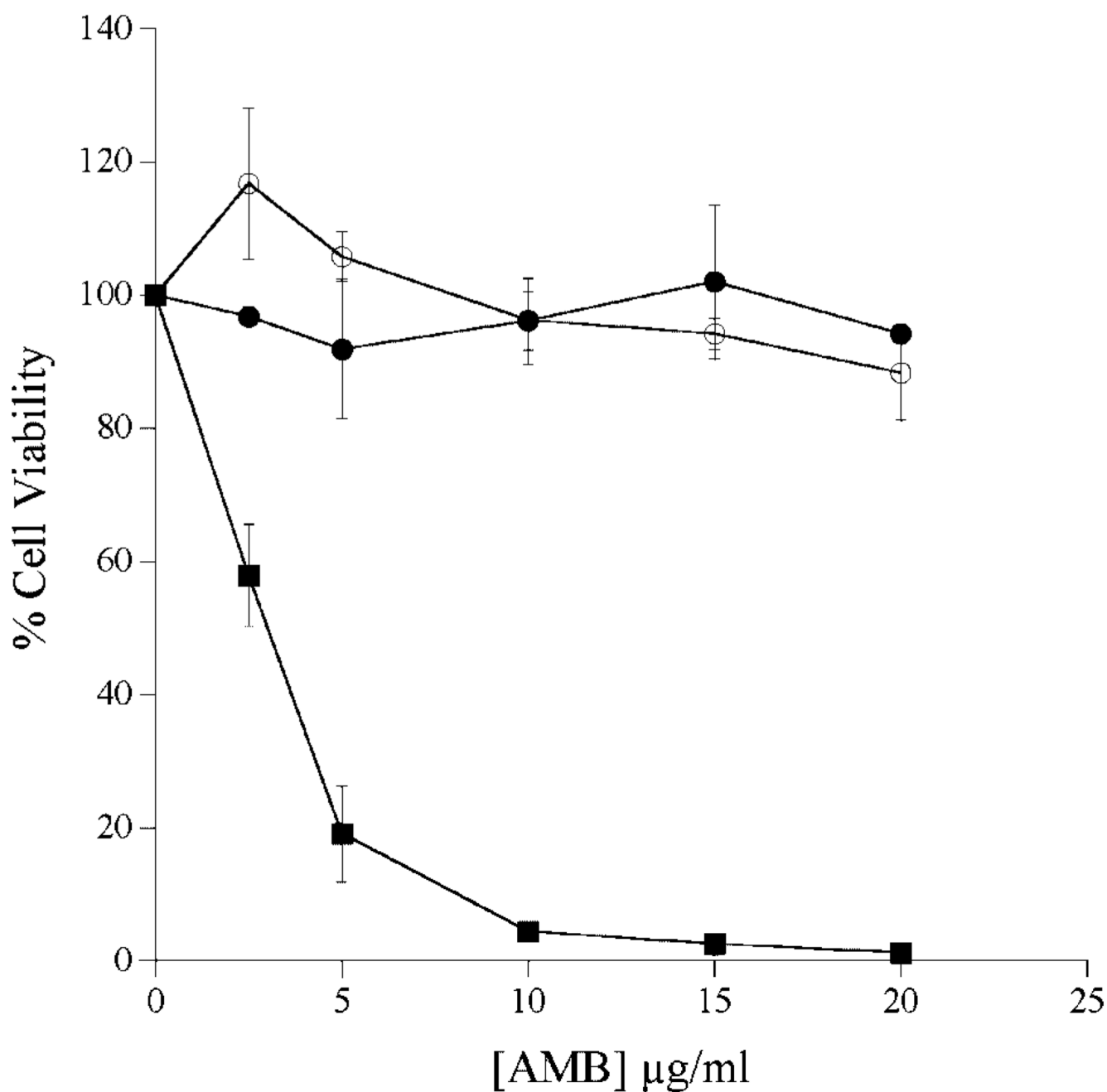


**Figure 5.** Effect of AMB on the viability of cultured Hep3B cells. Cultured Hep3B cells were treated with AMB at concentrations ranging from 0 to 20 µg/mL medium. After 24 h in the absence or presence of antibiotic, cell viability was measured using the MTT assay. Percentage cell viability was determined using the difference in absorbance (570 and 690 nm) at each AMB concentration. (Filled circles) ABLC; (open circles) ABLC-derived AMB-ND; filled squares, AMB-deoxycholate. Values reported are the mean  $\pm$  SD ( $n = 3$ ).

**Table 1**

## Effect of ApoA-I on AMB Solubility

<b>Formulation</b>	<b>Solubilization Efficiency<sup>a</sup></b>
Control ABLC	0.15 ± 0.05
Sonicated ABLC	10 ± 4.5
ABLC plus apoA-I	99.6 ± 0.40

<sup>a</sup>Solubilization Efficiency (%) = the amount of AMB in solution after centrifugation/AMB present initially × 100. All values reported are the mean ± SD (*n* = 3).

**Table 2**

Effect of AMB Lipid Formulation on Fungal Growth

Fungal Species <sup>b</sup>	IC <sub>90</sub> (µg/mL) <sup>a</sup>	
	AMB-ND	ABL-C
<i>A. fumigatus</i>	0.05 ± 0.02	0.03
<i>C. albicans</i>	0.03 ± 0.01	0.04 ± 0.02
<i>C. neoformans</i>	0.02	0.01

<sup>a</sup>IC<sub>90</sub> = concentration of ND that inhibited (greater than or equal to) 90% fungal growth. All values reported are the mean ± SD (*n* = 3). When not shown, standard deviation was zero.

<sup>b</sup>Fungi were cultured and growth determined as described in Materials and Methods Section.